

# Limits on the resolution of correlation PIV iterative methods

by

J. Nogueira, A. Lecuona and P. A. Rodríguez

Universidad Carlos III de Madrid, Department of Thermal and Fluids Engineering  
c/ Butarque 15, 28911-Leganés, Madrid, Spain.

E-Mail: goriba@ing.uc3m.es

## ABSTRACT

The spatial resolution of correlation Particle Image Velocimetry (PIV) still rises scientific interest, even though it is a frequently addressed issue. In conventional non-iterative PIV, the spatial resolution limits are of common knowledge (Willert and Gharib 1991 and Raffel *et al.* 1998, among others). On the contrary, advanced iterative methods that use image distortion present a more complex scenario. One of the concepts that rise more debate is the limiting effect of the interrogation window size. Some times the window size is considered as an absolute limitation for spatial resolution, but the sentence: "flow field fluctuations below the scale of the interrogation region can not be resolved" loses its validity when leading with iterative methods. Although these subjects have been addressed in the past (Nogueira *et al.* 1999), more details seem needed to fully explain the involved concepts. Consequently, a further description can be of interest. This paper focuses on the subject, trying to clarify key points about it. One example of the non well documented issues in this field is related to the application of a weighting function on the interrogation window grey levels. At first sight it seems that there is an "effective window size" associated to the weighting and the resolution limit could be thought as independent of the number of iterations. In this way the corresponding low-pass weighting would not be able to achieve a high spatial resolution. This is not the case. Figure 1 gives some hints about this. It shows the smoothing effect of the correlation PIV in a single processing pass with a common weighting function (figure 1c) and also gives the high resolution achieved with the same weighting after an iterative multi pass implementation with image deformation (figure 1d). The result points out the large improvement potential. This figure also shows that a resolution limit smaller than the size of the interrogation window is possible. The mathematical background behind these subjects is further developed in the paper.

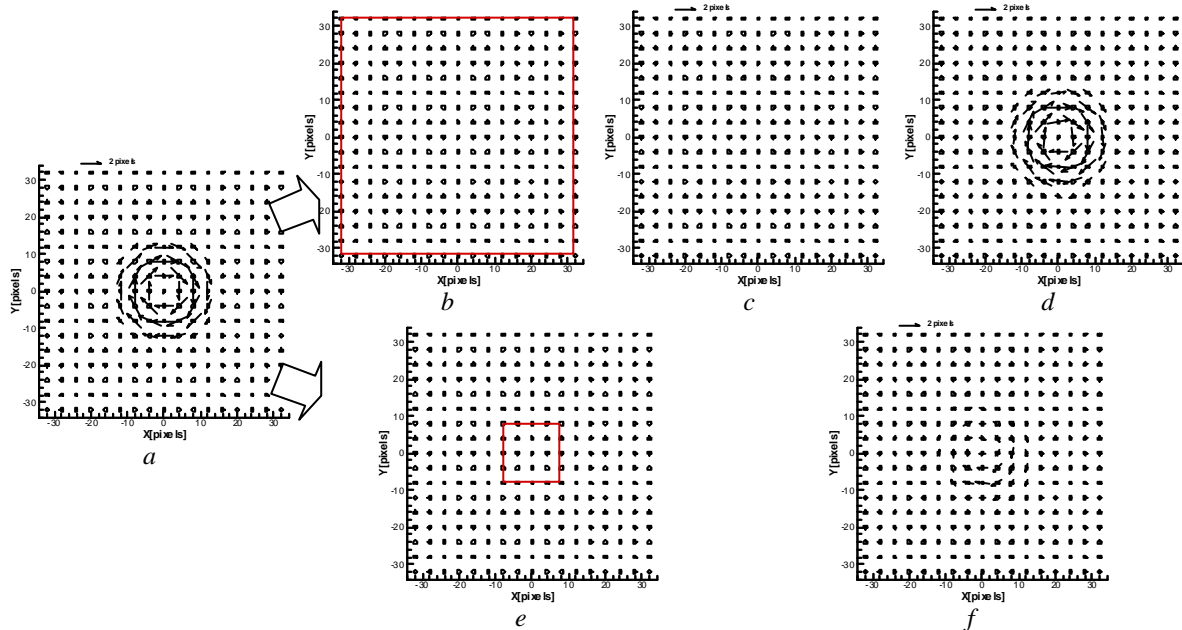


Fig. 1. Example of description of flow field features smaller than the size of the interrogation window, in pixels. The dots correspond to nodes of the vector grid. a) Vector field used to define a PIV couple of synthetic images. b) Size of a 64 by 64 pixels interrogation window weighted as figure 9 depicts. c) Vector field measured in a single pass implementation interrogation window in b. d) Vector field measured after a multi pass implementation of the interrogation window in b together with image distortion (130 iterations). e) Size of a 16 by 16 pixels interrogation window. f) Vector field measured with a single pass of a 16 by 16 pixels unweighted interrogation window.

In addition to that, the paper offers an analysis on the appropriate weighting functions for iterative processing, including the mathematical relation between the desired frequency response of the filter and the weighting function shape. This opens a line of work on possible weighting functions to develop, as the weightings used in these iterative methods, like LFCPIV (Nogueira *et al.* 1999), have not been optimised yet. As an example, an alternative weighting function is commented and tested on synthetic and real images as well.

## 1. INTRODUCTION

The first applications of digital PIV (Particle Image Velocimetry) were mainly focused on accurate descriptions of smooth flow fields (Willert and Gharib 1991) among others. This justifies the common tendency to evaluate PIV accuracy in fields of uniform displacements (Westerweel *et al.* 1997, Huang *et al.* 1997). In parallel to these implementations, the use of PIV on many industrial applications request more spatial resolution and the ability to cope with larger gradients as time passes (Raffel *et al.* 1992, Willert *et al.* 1996, Di Felice *et al.* 2001, Lecuona *et al.* 2004). In the beginning, these measurements in industrial facilities were performed at times sacrificing some accuracy. At present time, the development of advanced algorithms with increasing capabilities is allowing more accurate results.

Of these two requirements (i.e. spatial resolution and ability to cope with large displacement gradients) this paper focuses into the spatial resolution fundamentals for correlation based PIV. Reasoning about displacement gradients can be found elsewhere for conventional systems (Keane and Adrian 1993, Huang *et al.* 1993) among others, or advanced ones (Lecuona *et al.* 2004) among others.

The resolution limits of PIV has been an active subject for research for a long time. It is an important issue not only because of the desired ability to resolve small scales, but also because the non resolved scales may introduce noise in the measurement of larger ones. As mentioned in the abstract, Willert and Gharib (1991) already described the role of the interrogation window size on the spatial resolution of conventional correlation PIV methods with a single pass processing. This limit has been confirmed afterwards (Ullum *et al.* 1997, Raffel *et al.* 1998). On the other hand, Nogueira *et al.* (1999) showed that resolution far below the window size can be obtained in an iterative multi pass correlation PIV. The concept has motivated some interesting debate. This may be attributed to associating the spatial resolution limitation coming from the window size in single pass correlation PIV to a complete loss of information of smaller scales like it happens with a Nyquist sampling limit. The fact that a non usual weighting function is used in iterative methods that obtain resolution below the size of the interrogation window produces more confusion, as it can be considered as a reduction in the “effective window size” and thus producing the increase in resolution.

The results of this paper show that these are non appropriate concepts and that the limitation is related to the way the information is processed, more than to the window size itself. Section 3 shows that information of scales below the size of the interrogation window can be obtained independently of the existence of a weighting window. Additionally, that section explains the fundamental reason of using weighting functions in iterative algorithms and gives some designing rules for them. Section 4 shows a large weighted window that has a clear low-pass behaviour in respect to a smaller one. It also shows how the former one obtains better spatial resolution in an iterative procedure. Section 5 illustrates how “the effective size” when refereeing to robustness in industrial images (i. e. presence of outliers) is also larger for the weighted interrogation window. Along these sections, comparison of two differently weighted interrogation windows are also given for iterative PIV. Finally Section 6 draws some conclusions.

## 2. PHISICAL LIMITS FOR SPATIAL RESOLUTION IN PIV

Before dealing with other limitations it is convenient to highlight the role of two commonly accepted and recognised resolution limits. They are related to the mean distance between particle images in a PIV realization,  $\mathbf{d}$  and the distance between vectors in the PIV output,  $\mathbf{D}$ .

Both limits pay attention to the Nyquist sampling theorem. Namely, no information of higher frequencies than half the sampling frequency can be properly reconstructed due to lack of information. This applies to the spatial frequencies and results in an absolute impossibility to reconstruct information of characteristic length smaller than twice the distance of sampling.

In PIV two spatial samplings can be addressed:

- One is the sampling of the flow field by means of the particles seeded within it. These particles will give information on the velocity of the flow field in the point where they appear and thus not in a continuous way. The consequence of this is that the minimum wavelength that can be solved,  $\mathbf{I}_m$ , is related to the seeding density. In particular  $\mathbf{I}_m > 2\mathbf{d}$ . This mean distance between particles can be approximated by the number of particles images per unit surface in the PIV frame,  $N$ , expressed typically in particles per pixel (ppp):  $1/N \approx \mathbf{pd}^2/4$ .

Successful correlation PIV implementations have been reported on synthetic images with  $\mathbf{d} \sim 2$  pixels (0.32 ppp) (Nogueira *et al.* 2001, Lecuona *et al.* 2002) among others. Of course, if there is a high particle density with significant overlap of particles, the mean distance between information spots has to be considered instead, taking into account the diameter of the particles.

- The other spatial sampling is related to the vectors obtained as output of the PIV measurement or at intermediate steps in a multi pass algorithms. In both cases, it means a sampling of the continuous flow field, and any use of this sampled vector field implies an operation where the information of wavelengths smaller

than twice the distance between vectors is not available. If further iterations use the PIV image, the information of small wavelengths can be recovered if the distance between vectors is changed. This is because the PIV image incorporates all the wavelengths contained down to twice the mean distance between particles. Either if the vector distance is not changed for new iterations within the PIV measuring method or if it corresponds to the final output this second limit imposes  $I_m > 2D$ .

### 3. ALGORITHM RELATED LIMITS FOR SPATIAL RESOLUTION IN PIV

The size of the interrogation window has often been addressed as a resolution limit which is generally accepted for single pass conventional PIV. In addition to that, it can be found addressed as a Nyquist limit. This is a more compromising concept as a Nyquist limit implies an irreversible loss of information, as a result of aliasing small and large wavelengths. This section is focused on proving that the interrogation window is not an absolute limit nor it is forcedly associated to a Nyquist type limit. To achieve this, a reasoning is developed relying on a moving average processing algorithm instead of a PIV evaluation algorithm, as an ideal representation of it. The advantage of the moving average is its complete linearity in contrast to the non linearity associated to the particle displacement evaluation by a PIV straight algorithm, relevant when large particle displacement differences are found within the interrogation window (Nogueira *et al.* 2002, Lecuona *et al.* 2004). Further reasoning will concentrate on the PIV peculiarities in Section 4.

To illustrate the reasoning, a displacement field like the one depicted in figure 2a has been chosen. Figure 2b shows the detailed displacement field to measure and the size of the interrogation window along the  $y$  axis.

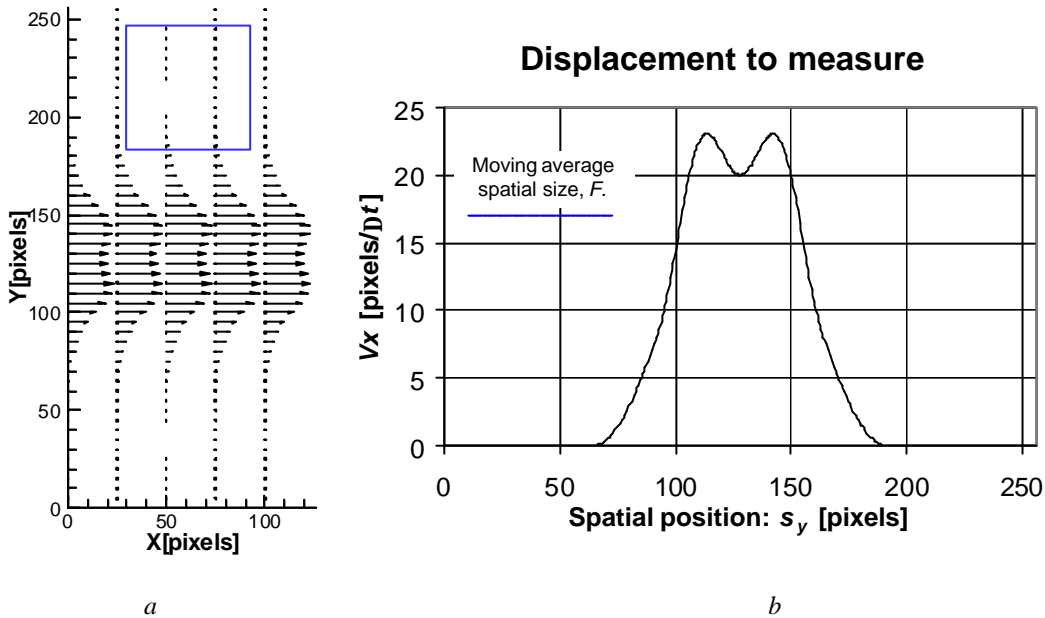


Fig. 2 Test vector field. a) 2D layout (the blue square indicates the size of the interrogation window). b) Detailed profile along a vertical line (the blue horizontal line segment indicates the size of the interrogation window).

The vector distance in figure 2a is large only for display purposes. The information is available for every single pixel, meaning this a Nyquist limitation based on  $d$  or  $D$  only for wavelengths smaller than 2 pixels. A moving average related to an interrogation window of 63 by 63 pixels has been implemented on this vector field. The resulting displacement field is detailed in figure 3a. Figure 3b depicts the resulting displacement field. Extracting the different spatial wavelengths in the measurement, relative errors are larger than 10% for spatial wavelengths smaller than  $I = 252$  pixels (four times the size of the interrogation window). Reducing the relative errors limit to 2.5% the wavelength limiting value would grow up to  $I = 510$  pixels (about eight times the size of the interrogation window). Even with this large amount of error in the moving average measurement, the following subsection shows that it is not due to a Nyquist type limitation, and that all the information for wavelengths smaller than the size of the interrogation window can be recovered using only the measurement itself.

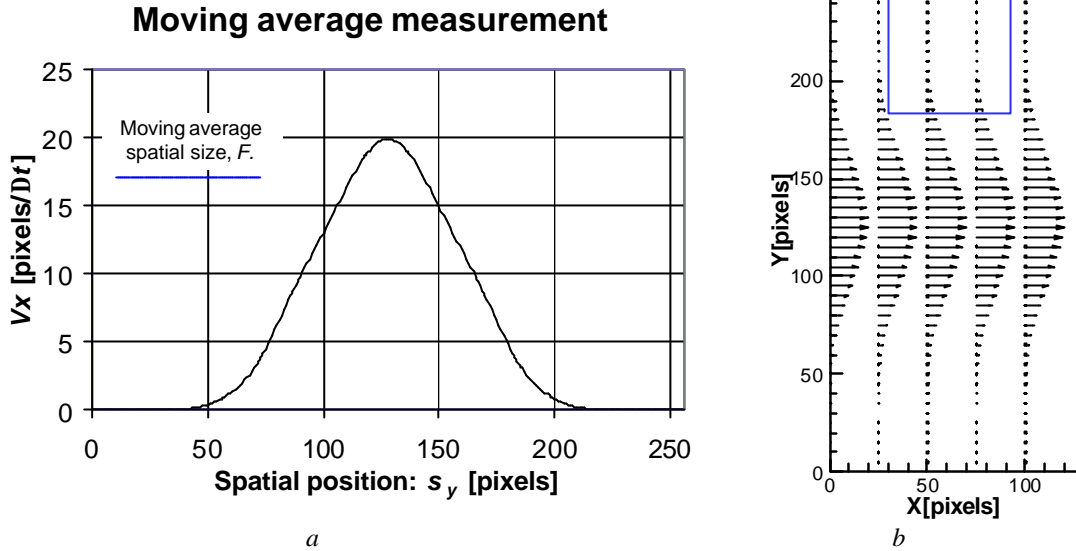


Fig. 3 Moving average measurement on the test vector field depicted in figure 2. a) Detailed profile of the measurement along a vertical line (the blue segment indicates the size of the interrogation window). b). 2D layout (the blue square indicates the size of the interrogation window).

### **3.1 Recovering information from wavelengths smaller than the size of the interrogation window in a non iterative algorithm.**

The fact that the application of the moving average is not related with an irreversible loss of information like in the Nyquist case can be checked as follows: the frequency response of a moving average (i.e. the amplification of each spatial wavelength when measuring with a moving average) is a known function. What we have obtained in figure 3 is associated to multiplying the amplitude associated to each wavelength present in figure 2 by this frequency response. In consequence, we can invert this process by dividing the amplitude associated to each wavelength present in figure 3 by the corresponding frequency response. Finally the inverse Fourier transform of the resulting values is calculated.

Figure 4 illustrates this procedure. The result is that the original function is fully reconstructed using the moving average measurement. This indicates that all the information of the original function is contained in the moving average measurement, it is not lost and it can be deconvolved unlike the Nyquist associated aliasing.

In the case depicted in figure 4, all these operations have been performed over a discrete sampling with  $D = 1$  pixel. The result is the reconstruction of the original displacement field with errors smaller than 0.004 pixels. The relative error associated to the amplitude of the different wavelengths is smaller than 2.5% for  $I > 8$  pixels and smaller than 10% for  $I > 4.2$  pixels (less than the fifteenth part of the interrogation window). These errors are coherent with the discretization of  $D = 1$  pixel.

This result is partly due to the perfect linearity of the moving average. Frequencies in which the moving average has a zero frequency response are singular points that would loose the information in that very particular points.

The objective of this subsection is just to indicate that a large interrogation window does not mean necessarily a loss of information for small wavelengths. This loss, when present, is associated to other concepts. In the particular case of PIV, there might be a loss of information in the non-linear operations when calculating the displacements. In particular, it is found in the correlation domain where the peak of the most likely displacement is searched and its maximum located by fitting a function. The information from some particle pairs within the interrogation window that do not contribute to the main peak width is lost. This loss would only happen when the skirt of the peak, corresponding to these particles pairs, do not reach the main function-fitted peak. Obviously, these will be much more dependent on the magnitude of the displacement differences in respect to the particle size than to the size of the interrogation window itself (Nogueira *et al.* 2002, Lecuona *et al.* 2004).

The favourable case in which all the displacements contribute to the shape of the main peak is usually fulfilled if the applicability restrictions from Keane and Adrian (1993) are met. Nevertheless, even in this case, the precise frequency response of PIV would be complex and not easy to describe. Furthermore, noise in the measurement has to be taken into account. These facts give sense to searching a way to deconvolve the information from different wavelengths in a way that would not need the knowledge of the frequency response. The following subsection is focused on this.

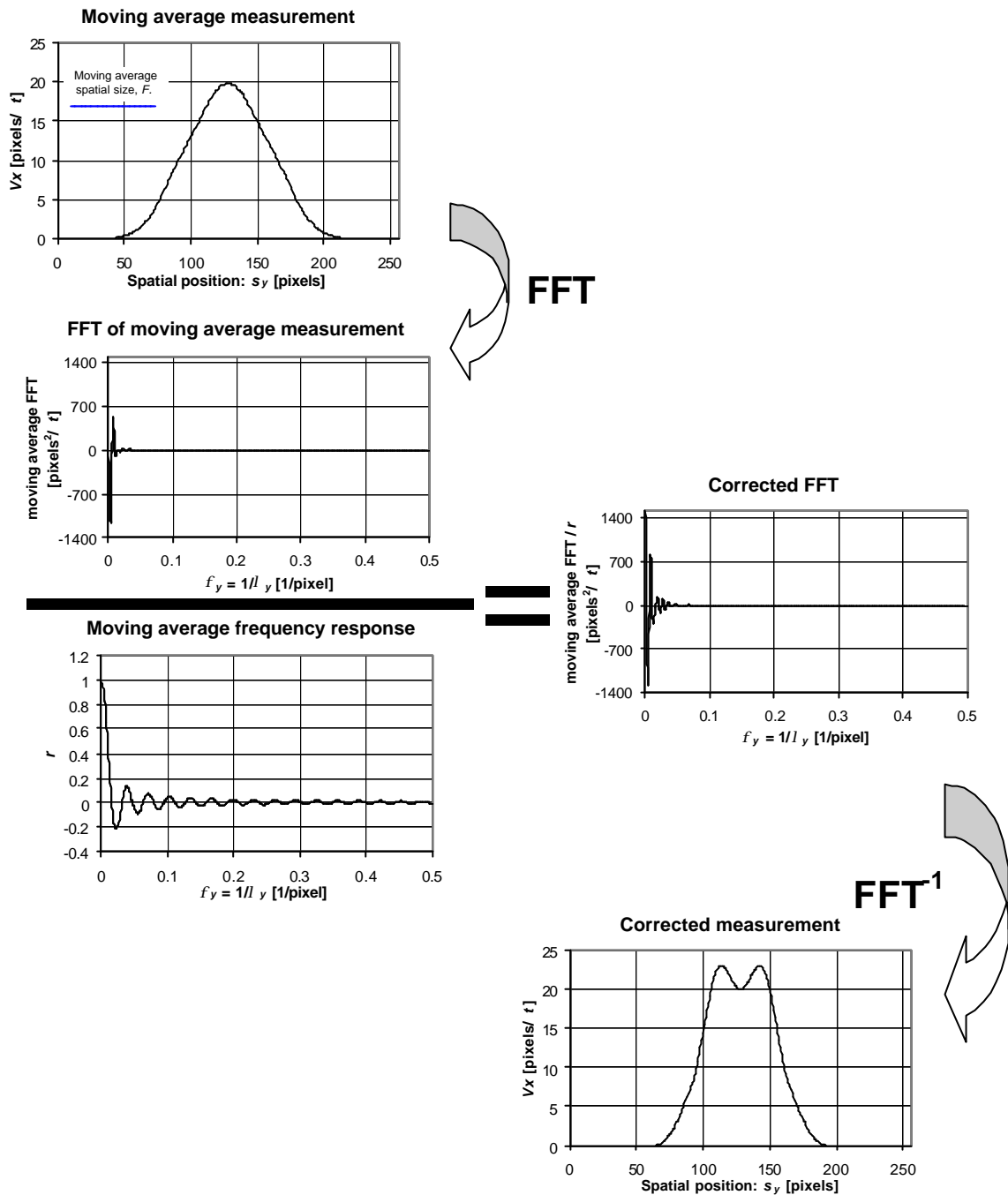


Fig. 4 Example showing that most of the information on spatial wavelengths smaller than the interrogation window can be recovered in a moving average.

### 3.2 Recovering information from wavelengths smaller than the size of the interrogation window in an iterative algorithm.

Once it has been established that large interrogation windows are able, at least to partially discriminate information from small wavelengths, the possibility to iteratively correct the measurement is open, specially when the moving average-like linear regime is approached as this correction progresses. The basic idea is to subtract the measurement to the real information to obtain a measure of the error. Successive measurements of the error would eventually reduce it to an acceptable low level. In the first steps large wavelengths would converge to a correct measurement and, afterwards, the error in smaller wavelengths would decrease. The iterative procedure would perform the following steps:

1. Measurement of the flow field.
2. Subtraction of the measurement to the real displacement to obtain the error. As an example, in the case of PIV, this subtraction can be performed by distorting the original images to compensate the measured

- displacement field. It should be observed that the resulting information that contains the error is not directly available. It is contained in a new couple of images that have to be processed.
3. Measurement of this error (on the new couple of images in a PIV procedure).
  4. Correction of the measurement from the first step by adding that measurement and the actual measurement of the error.
  5. Proceed through steps 2-4 iteratively until convergence.

This scheme is sketched in figure 5. In that figure the result associated to a certain wavelength with frequency response  $r$  is made explicit.

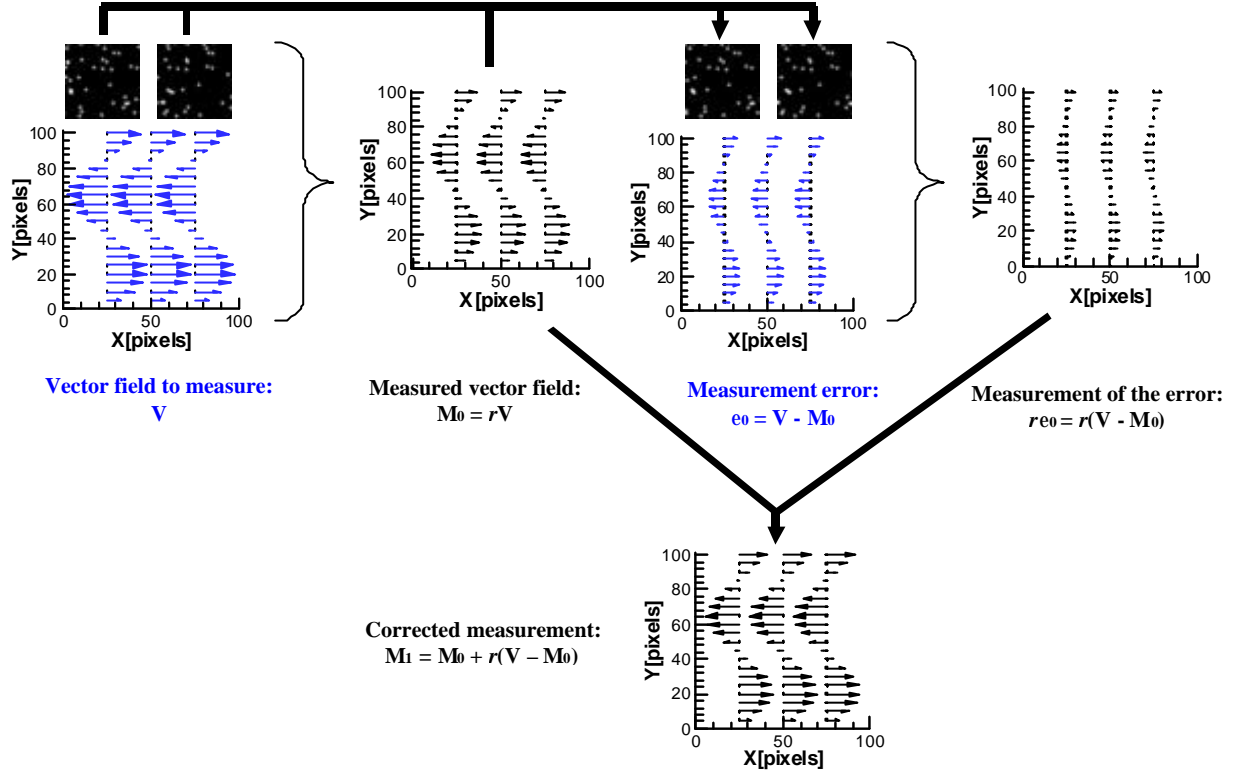


Fig. 5 Scheme of the iterative procedure to correct a measurement. The information in blue indicates data that is contained in a couple of images in the case of PIV (i. e. it is not directly available).

Following the previous steps and through the reasoning and nomenclature in figure 5, for the  $n$ -th iteration the corrected measurement corresponds to:  $M_n = M_{n-1} + r(V - M_{n-1})$ . Taking into account the value of  $M_i$  along the different corrections, this expression can be rewritten as:  $M_n = V - V(1 - r)^n$ .

It can be observed that the convergence is only obtained when the frequency response satisfies:  $2 > r > 0$ . Going back to the moving average frequency response, this is not the case for every frequency (see figure 6a). Fortunately there is an easy way of changing the frequency response of an average and that is to weight it. The only restriction now is to find a weighting that produces a frequency response contained in that interval, between 2 and 0. The ratio between the shape of a weighting function,  $u^2$ , and the frequency response that it produces,  $r$ , is presented in expression (1). The detailed reasoning can be read elsewhere (Nogueira 1997).

$$u^2 = \sum_{i,j=0}^{\infty} m_{ij} \cos\left(\frac{2pix}{F}\right) \cos\left(\frac{2pjy}{F}\right) \Leftrightarrow r = \frac{\text{sen}(pf_x F) \text{sen}(pf_y F)}{pf_x F \cdot pf_y F} \sum_{i,j=0}^{\infty} m_{ij} (-1)^{i+j} \frac{f_x^2 F^2}{f_x^2 F^2 - i^2} \cdot \frac{f_y^2 F^2}{f_y^2 F^2 - j^2} \quad (1)$$

Where  $x$  and  $y$  are spatial coordinates measured from the center of the interrogation window.  $m_{ij}$  are the set of coefficients of a symmetrical Fourier expansion that defines the weighting function. In this expansion, the following additions of coefficients should be null to account for the finite length of the interrogation window:  $\sum m_{ij} (-1)^i = 0$  along  $i$ ,  $\sum m_{ij} (-1)^j = 0$  along  $j$ . The expression of the frequency response indicates that all these coefficients  $m_{ij}$  should be positive for  $r$  to be positive all along the spatial frequencies. This is a necessary condition but is not sufficient. In addition to that,  $r$  has to be checked in order to assure this property.

Once that expression (1) is obtained, the immediate temptation could be to search for a set of coefficients that would make  $r = 1$  for every wavelength. Of course, this weighting function corresponds to a Dirac delta function that would be impossible to implement in PIV as it corresponds to an differentially small interrogation window side. In consequence, a function with a more gentle decrease towards zero should be searched. An arbitrarily

chosen weighting that satisfies these criteria for 1D corresponds to expression (2) and gives the frequency response that is depicted in figure 6b, for the moving average of 63 pixels linear size.

$$u^2 = 3 \left( 4 \left| \frac{y}{F} \right|^2 - 4 \left| \frac{y}{F} \right| + 1 \right); \quad r = \frac{6}{p^2 f_y^2 F^2} \left( 1 - \frac{\sin(p f_y F)}{p f_y F} \right) \quad (2)$$

In this expression, like in expression (1),  $y$  corresponds to the linear coordinate measured from the center of the interrogation window.

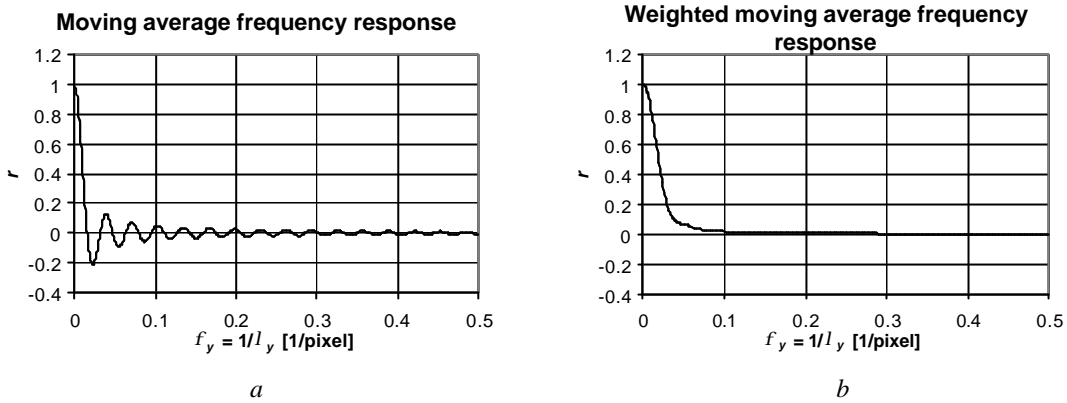


Fig. 6 Effect of a weighting in the frequency response. a) Frequency response of a 63 pixels wide moving average. b) Frequency response of a 63 pixels wide moving average weighted with expression (2).

Using this weighting function, the iterative algorithm previously commented can be tried on the test displacement field of figure 2. The iterative algorithm has been implemented with the unweighted moving average to check for the lack of convergence when the frequency response is not contained in the interval from 0 to 2. The results are depicted in figure 7. In the case of weighted moving average, the result in the first iteration produces a clearly low-pass measurement. After 20 iterations, the error in the different wavelengths is smaller than 10% for  $I > 28$  pixels (as would correspond to a 7 pixels size moving average). After 40 iterations, this error is smaller than 10% for  $I > 18$  pixels (as would correspond to a 4.5 pixels size moving average). For the case that proves the lack of convergence of the unweighted moving average, the result is unsatisfactory, as expected.

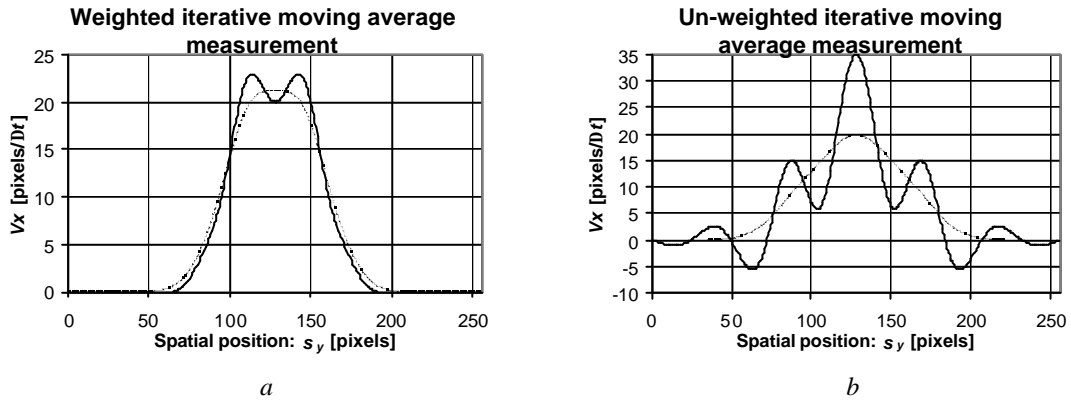


Fig. 7 Measurement of the test field in figure 2 by means of the iterative procedure commented in the text. a) Iterative procedure with a weighted moving average (expression(2)). Thin discontinuous line corresponds to first iteration. Thick continuous line corresponds to 20<sup>th</sup> iteration. b) Iterative procedure with an unweighted moving average. Thin discontinuous line corresponds to first iteration. Thick continuous line corresponds to 10<sup>th</sup> iteration.

Once again, if we consider the case of PIV instead of that of the moving average, the frequency response is *a priori* unknown. Moreover, it is clearly non-linear; in particular, the response to a certain wavelength can produce a contain at other wavelengths. Generally these wavelengths are smaller than the original one. As the frequency response is larger for larger wavelengths, it is reasonable to suppose that as they converge they would stop introducing spurious contain in the smaller ones. This together with the fact that the iterative algorithm is so robust as to converge even with responses above unity gives an acceptable indication in the sense that it could work with PIV evaluations. The following section is related to this implementation.

#### 4. APPLICATION OF THE ITERATIVE ALGORITHM TO SYNTHETIC IMAGES

The way to implement a weighting filter in PIV is not straight ahead. As an example, normalization when computing the correlation can be used or considered as little contributing. In this case the implementation follows the steps detailed in Nogueira *et al.* 2001.

In this section two weighting function are tested on interrogation windows of 64 by 64 pixels. One corresponds to the previous reference, it is a two dimensional extension of the one in expression (2) and is defined by expression (3).

$$\mathbf{u}^2 = 9 \left( 4 \left| \frac{x}{F} \right|^2 - 4 \left| \frac{x}{F} \right| + 1 \right) \left( 4 \left| \frac{y}{F} \right|^2 - 4 \left| \frac{y}{F} \right| + 1 \right) \quad (3)$$

The other weighting is an axial symmetric version that could improve the measurements by reducing the directional anisotropy of the function. It is defined by expression (4). Both functions are depicted in figure 8.

$$\mathbf{u}^2 = \frac{24}{p} \left( 4 \left| \frac{\sqrt{x^2 + y^2}}{F} \right|^2 - 4 \left| \frac{\sqrt{x^2 + y^2}}{F} \right| + 1 \right) \quad \text{if } \left| \frac{\sqrt{x^2 + y^2}}{F} \right| < 0.5; \quad \mathbf{u}^2 = 0 \text{ otherwise} \quad (4)$$

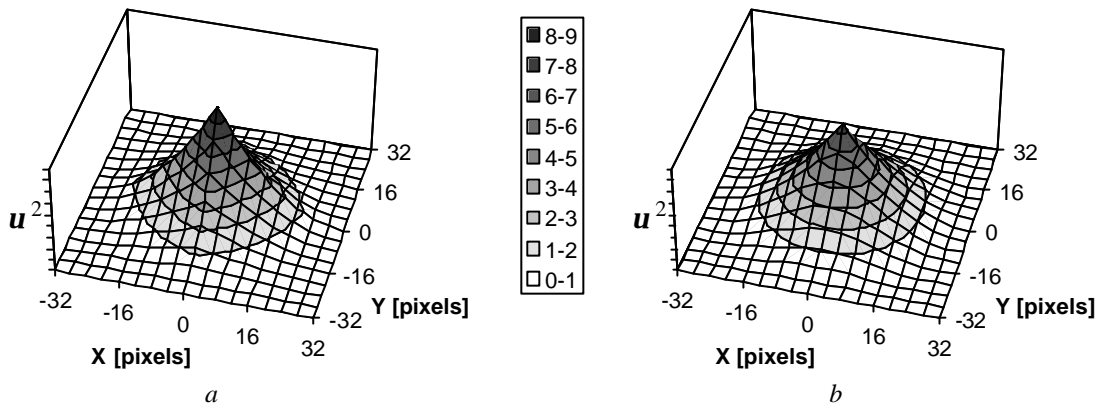


Fig. 8 Shapes of the implemented weighting functions. a) Weighting function from expression (3). b) Weighting function from expression (4).

Synthetic images were purposely designed to test the spatial resolving performance of these weightings. They contain no noise except for the spatial discretisation of the simulated image sensor and the usual effective 8 bit gray level sampling. The average distance between the randomly located particle images is small,  $d = 2$  pixels, i.e.  $4/(p \cdot d) \approx 0.3$  ppp. The  $e^{-2}$  diameter of all the Gaussian particle images is  $d = 2$  pixels. The Gaussian shape of the particle images was integrated with unity fill factor over each square pixel surface (Westerweel 1998). Constant intensity profile was selected for the light sheet, so that each particle can equally contribute to the correlation. Where particles overlap, the corresponding intensities were added. The associated particle surface density is on the edge where speckle pattern starts to appear, but this phenomenon will not be taken into account in this paper. The rationale behind the high density chosen is to reduce the error coming from the sampling of the flow field and more clearly reveal the differences between both filters. On the other hand, the resulting images look very similar to real ones obtained in wind tunnels, being the particle surface density similar. Grey level saturation resulted to be statistically insignificant. No out of plane displacement was considered. In some cases this kind of images have been used by the authors, like Lecuona *et al.* (2002 and 2004).

The test displacement field implemented in these images corresponds to a vortex of no radial displacement and an azimuthal displacement of  $2.4 \cdot \sin(pR/16)$  for  $R < 16$  pixels and null otherwise.  $R$  is the distance from the center of the image. The resulting vector field is depicted in figure 1a. This produces a feature that is clearly smaller than the weighted interrogation windows (see figure 1b). To check that the weighted interrogation windows are still low-pass when compared with clearly smaller windows, a 16 by 16 pixels interrogation window is depicted in figure 1e. The measurement that it produces (figure 1f) is clearly less low-pass than the measurement obtained after one pass of a weighted interrogation window (figure 1c). Nevertheless, the proposed iterative procedure clearly recovers small wavelength features after a large number of iterations (figure d).

The root mean square value of the error,  $rms(e)$ , over the whole PIV measurement has been normalized with that of the flow field displacements  $rms(s)$  for the three measurements. It is depicted in figure 9. It can be observed that the weighted windows outperform the small interrogation window after 12 to 14 iterations. After a hundred of iterations the error is ten times smaller for the large iterative windows.



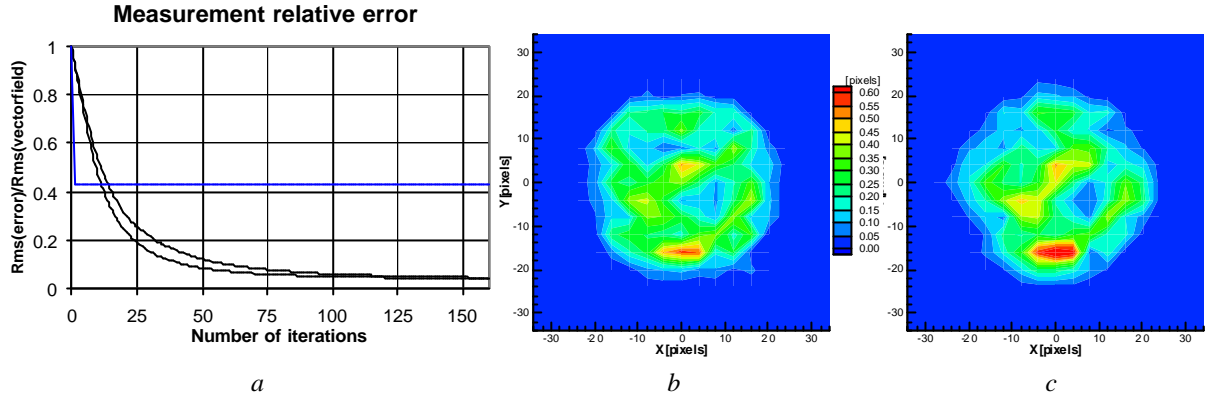


Fig. 9 Error behaviour in the different tests. a) Evolution of the error with the number of iterations. The lower black curve corresponds to the weighting function from expression (3) and the upper black one to expression (4). The blue horizontal line corresponds to the 16 by 16 pixels un-weighted interrogation window (only one iteration). b) Error corresponding to the weighting function from expression (3) after 160 iterations. c) same as b but for expression (4).

Figure 9b and figure 9c show a comparison between the final results when using the weighting functions defined in expressions (3) and (4). The axial-symmetric filter shows a slightly larger error but a more isotropic behaviour.

These two weighting filters show little differences, but the designing rules given when commenting expression (2) allow for much larger differences. An example of weighting design would be one with a special response sensitivity to a certain frequency. This would be achieved by increasing the corresponding  $m_j$  and changing the rest of them in order to fulfil  $\sum m_j(-1)^j = 0$  along  $i$ ,  $\sum m_j(-1)^j = 0$  along  $j$ . Use of this weighting should be done with care as the convergence would happen for certain frequencies before some others.

## 5. APPLICATION OF THE ITERATIVE ALGORITHM TO REAL IMAGES

The previous section deals with synthetic PIV images. This is useful because in those images the displacement field is completely known. But the objective of PIV algorithms are real images. Although the flow field in a real image is unknown, tests are customary for checking the coherence between the results obtained from synthetic images and those from real ones obtained in an industrial facility. In addition to the comparison between the two weighting functions proposed, the real images will help in this case to test the robustness of the weighted interrogation windows within the proposed iterative method.

The images chosen for this test correspond to a couple of PIV images from a measurement campaign carried out by DLR and Airbus within the Europiv2 consortium (Arnott *et al.* 2004). The test campaign focused on the 2D low Mach number aerodynamics around a wing profile in high lift configuration. figure 10a gives a sketch of the configuration and the position chosen for the image analyzed in this section. Another example (ref: 456\_18\_c3\_0020.b16.) from this test campaign can be found in Lecuona *et al.* (2004). This couple of images is an easier case than the one in the mentioned reference but still a difficult one where typical commercial state-of-the-art software had problems in correctly evaluating the flow field. The software used for comparison implements conventional PIV plus integer window offset. The window offset was refined by means of a three steps multigrad scheme. The purpose of the first two steps is to locally determine an accurate value for integer window offset for the third one. No image deformation was used, and window sizes  $F$  were 128, 64 and 32 pixels in the three successive steps. Between steps a validation algorithm was implemented, rejecting vectors that differed more than 45% of the local median of a 3 by 3 neighborhood. The resulting vorticity field is plotted in figure 10b.

On the same PIV image pair, LFCPIV was applied following the algorithms described in Nogueira *et al.* (2001) and Lecuona *et al.* (2002) giving the results presented in figure 10c. The same procedure but with the axial-symmetric filter from expression (4) gives the results plotted in figure 10d. In both realizations, the Von K arman vortex street in the wake of the slat is clearly visible and also there is much less spurious results than with conventional PIV. They are easily detected because of the inverse vorticity structure appearing at both sides of the spurious vector.

This robustness is of great importance when processing images coming from industrial-like setups. It supports the use of large windows at the cost of a higher computing time of the associated iterations.

About the comparison of the two weighting functions proposed in this paper, it can be observed that both perform satisfactorily. Checking the results in detail, it seems like the axial-symmetric one gives better results on the boundary layer over the profile but is slightly less robust in places with light intensity discontinuities. These differences are too small to consider one better than the other. So both options seem suitable from this viewpoint.

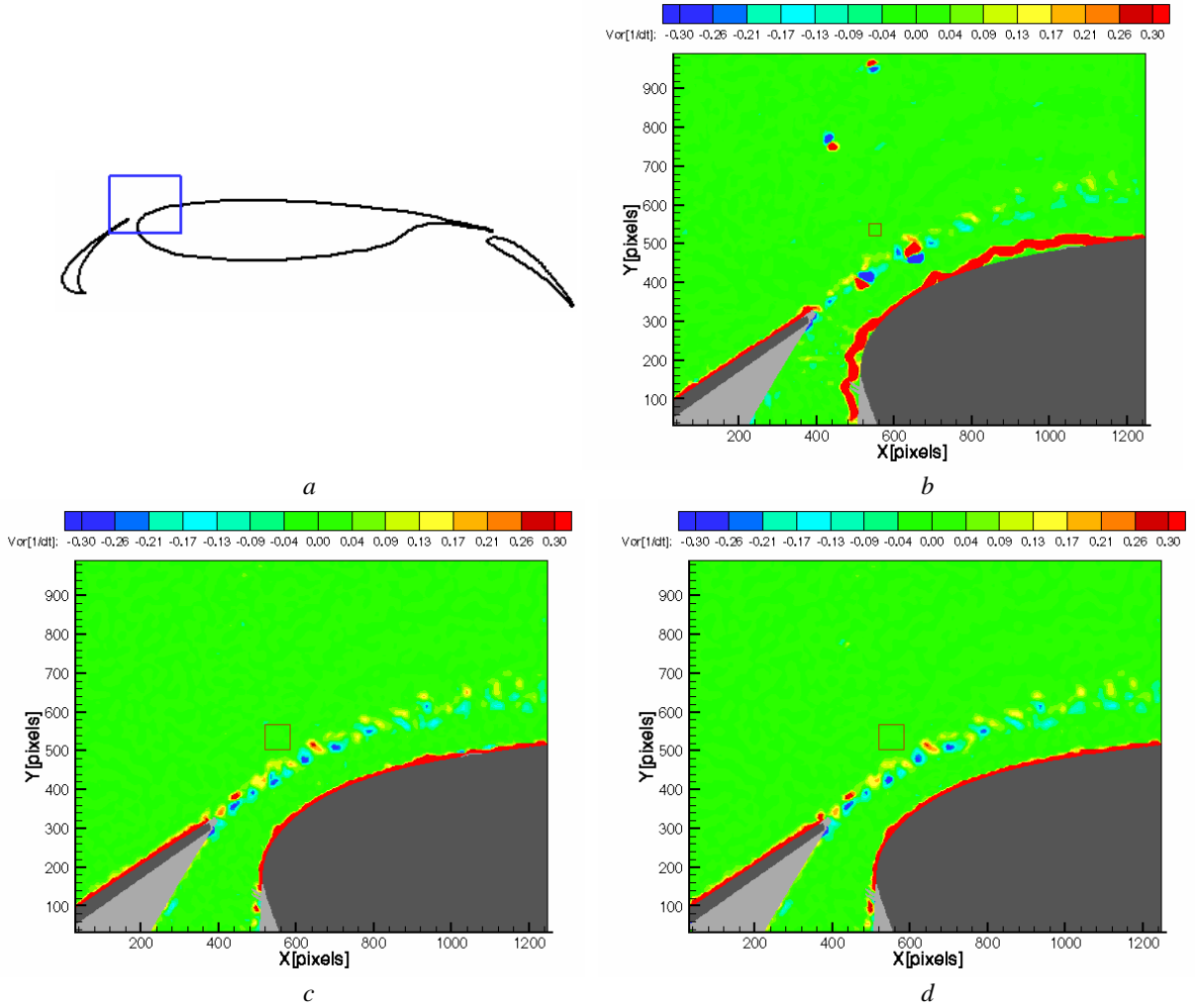


*Fig. 10 Performance comparison on real images from an industrial facility. Dark grey means solid objects; light grey means places where reflections and shadows suppress all data. a) Location of the PIV image analyzed in this section. DLR ref: 101112\_12\_c3\_0010.b16. b) Vorticity plot obtained from conventional PIV data. The size of the interrogation window (32 by 32 pixels) is indicated by a brown box. c) Same as b but for the 64 by 64 weighted interrogation window weighted by expression (3). d) same as c but using expression (4).*

## 6. CONCLUSIONS

This paper concludes that the interrogation windows in PIV can contain useful information of wavelengths clearly smaller than its size.

Additionally, this size is not a limitation for spatial resolution in iterative multi pass PIV when using the suitable weighting function.

Conditions for the suitability in terms of convergence in the iteration are given.

The use of the weighting functions do not avoid the low-pass behaviour of the interrogation window but modulates the frequency response in a way that allows for iterative reconstruction of the information contained at small wavelengths.

The robustness (i. e. ability to avoid outliers) of a weighted interrogation window within the iterative procedure used in this paper can be higher than that of smaller windows. Thus, combining better resolution with higher robustness.

The rules for designing weighting functions for iterative algorithms are given in the paper. This opens a line of work as these filters have not been optimised in the past.

## AKNOWLEDGMENTS

This work has been partially funded by the COJEN European project, Specific Targeted RESEARCH Project EU Contract No. AST3-CT-2003-502790; the Spanish Research Agency grant AMB1999-0211, DPI2000-1839-CE,

## REFERENCES.

- Arnott AD, Schneider G, Neitzke K-P, Agocs J, Schröder A, Sammler B and Jompenhans J. (2004) “Detailed characterization, using PIV, of the flow around an aerofoil in high-lift configuration”, Proceedings of the EUROPIV 2 Workshop on Particle Image Velocimetry. Editors: Stanislas M, Westerweel J, Kompenhans J. Springer Verlag.
- Di Felice F, Felli M, De Gregorio F (2001). “Ship model wake analysis by means of PIV in large Circulating Water Channel”, *Int. J. of Offshore and Polar Engineering*, 11 (4): pp. 261-266.
- Huang H, Dabiri D, Gharib M (1997). “On errors of digital particle image velocimetry”, *Meas. Sci. & Technol*, 8: pp. 1427-1440.
- Huang HT, Fiedler HE, Wang JJ (1993). “Limitation and Improvement of PIV Part I: limitation of conventional techniques due to deformation of particle patterns”, *Exp. Fluids*, 15: pp. 168-174.
- Keane R D, Adrian R J (1993). “Theory of cross-correlation of PIV images”, Nieuwstadt FTM (ed). *Flow Vis. and image Analysis*. Dordecht: Kluwer Academic, pp. 1-25.
- Lecuona A, Nogueira J, Rodríguez PA, Santana D (2002). “Accuracy and time performance of different schemes of the local field correction PIV technique”, *Exp. in Fluids*, 33 pp 743–751.
- Lecuona A, Nogueira J, Rodríguez PA, Acosta A (1994). “PIV evaluation algorithms for industrial applications” *Meas. Sci. and Technol.*, 15 (6): pp. 1027 – 1038.
- Nogueira J (1997) “Contribuciones a la técnica de velocimetría por imagen de partículas (PIV)”, PhD Thesis E. T. S. I. Aeronáuticos, Universidad Politécnica de Madrid, Spain.
- Nogueira J, Lecuona A, Rodríguez PA (1999). “Local Field Correction PIV: On the increase of accuracy of digital PIV systems”. *Exp. Fluids*, 27/2: pp. 107-116.
- Nogueira J, Lecuona A, Rodríguez PA (2001). “Local field correction PIV, implemented by means of simple algorithms and multigrid versions”, *Meas. Sci. Technol.*, 12: pp. 1911-1921.
- Nogueira J, Lecuona A Ruiz-Rivas and Rodríguez P A (2002) “Analysis and alternatives in two-dimensional multigrid particle image velocimetry methods: application of a dedicated weighting function and symmetric direct correlation”, *Meas. Sci. Technol*, 13: pp. 963-974.
- Raffel M, Leidl B, J Kompenhans (1992). “Data validation for particle image velocimetry”. 6th Int. Symp. on Appl. of Laser Techniques to Fluid Mechanics, Lisbon, Portugal, July 20-23.
- Raffel M, Willert CE and Kompenhans J (1998). “Particle Image Velocimetry: A Practical Guide”, ISBN 3-540-63683-8 Springer-Verlag.
- Ullum U; Schmidt J J; Larsen P S and McCluskey D R (1997). “Statistical analysis and accuracy of PIV data”, *Int. Workshop PIV’97-Fukui*, Fukui, Japan. July 1997.
- Westerweel J; Dabiri D; Gharib M (1997). “The effect of a discrete window offset on the accuracy of cross-correlation analysis of digital PIV recordings”, *Exp. Fluids*, 23: 20-28.
- Westerweel J (1998). “Effect of sensor geometry on the performance of PIV”, 9th Int. Symp. on Applications of Laser Techniques to Fluid Mechanics. Instituto Superior Técnico, Lisbon, Portugal.
- Willert CE; Gharib M (1991). “Digital particle image velocimetry”, *Exp. in Fluids*, 10: pp. 181-193.
- Willert C, Raffel M, Kompenhans J, Stasicki B, Kahler C (1996). “Recent applications of particle image velocimetry in aerodynamic research”, *Flow Meas. and Instrum.*, 7 (3-4): pp. 247-256